The C_8H_8 Radical Cations of Cyclooctatetraene, Semibullvalene, and Their Common Bisallylic Rearrangement Product: Electronic Structure and Potential Energy Surfaces

Thomas Bally,*,† Leo Truttmann,†,§ Sheng Dai,‡,⊥ and Ffrancon Williams‡

Contribution from the Institute of Physical Chemistry, University of Fribourg, Pérolles, CH-1700 Fribourg, Switzerland, and Department of Chemistry, University of Tennessee, Knoxville, Tennessee 37996-1600

Received March 15, 1995[⊗]

Abstract: The recently discovered access paths to the radical cation of bicyclo[3.3.0]octa-2,6-diene-4,8-diyl ($BOD^{\bullet+}$) are explored by electronic absorption (EA) spectroscopy whereby previous ESR results are confirmed. The electronic and molecular structure of $BOD^{\bullet+}$ and of its photoprecursor, the radical cation of cyclooctatetraene ($COT^{\bullet+}$), are discussed on the basis of their EA spectra and ab initio calculations. The ground and excited state potential surfaces common to the title cations are explored, and it is shown that the $COT^{\bullet+} \rightarrow BOD^{\bullet+}$ photorearrangement proceeds mainly by virtue of a pronounced Jahn-Teller distortion of the second excited state of $COT^{\bullet+}$ (^2E). This distortion competes effectively with internal conversion to the first excited state, leads to an inversion of the ground state symmetry, and covers a substantial part of the reaction path leading to the bisallylic cation.

1. Introduction

Valence isomers of annulenes, in particular the C_8H_8 group of compounds, undergo many interesting photochemical, thermal, and catalytic interconversions.[1] Recent advances in radical ion (photo)chemistry have added a new facet to the investigation of such processes, because after ionization, novel species become accessible which have no stable counterparts on the corresponding neutral hypersurfaces.[2]

Recently, Williams et al. have used ESR spectroscopy to explain the enigmatic photochromism of ionized 1,3,5,7-cyclooctatetraene (COT)[3a] which had been observed some time ago by Shida and Iwata.[4] They found that the previously unidentified photoproduct is identical to the species obtained upon ionization of semibullvalene (SBV) and assigned to the oxidized form of the bisallylic biradical, bicyclo[3.3.0]octa-2,6-diene-4,8-diyl (BOD).[3b]

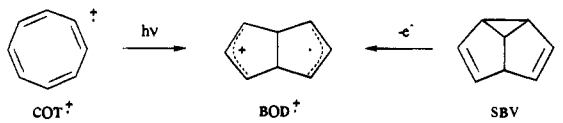

Our interest in the electronic structure and photochemistry of organic radical ions[5] led us to look at the above species in some more detail in order to arrive at an understanding of their electronic structure and consequently the mechanisms of their interconversions. The latter point has already been discussed qualitatively by Williams et al.[3] who pointed out that both the thermal $SBV^{\bullet+} \rightarrow BOD^{\bullet+}$ as well as the photochemical $COT^{\bullet+} \rightarrow BOD^{\bullet+}$ rearrangement are formally symmetry-allowed processes, whereas the ground state $COT^{\bullet+} \rightarrow BOD^{\bullet+}$ reaction is symmetry forbidden. However, a complete understanding of the above reactions seemed to require a full exploration of the processes along the respective reaction coordinates.

This paper describes the results of a study on the electronic structure of the title C_8H_8 radical cations and the potential surfaces interconnecting them. We believe that this has led us to a better understanding of the nature of the three species and the pericyclic processes by which $BOD^{\bullet+}$ is formed. In particular we discuss the degree of planarization induced by ionization of COT and we show that the formally symmetry-allowed $COT^{\bullet+} \rightarrow BOD^{\bullet+}$ photoreaction is driven by a pronounced Jahn-Teller distortion of electronically excited $COT^{\bullet+}$.

2. Electronic Absorption (EA) and Electron Spin Resonance (ESR) Spectra

Figure 1 shows the EA spectra observed during a stepwise photochemical transformation of $COT^{\bullet+}$ (λ_{max} = 505 nm) to $BOD^{\bullet+}$ (λ_{max} = 635 and 397 nm) in a Freon matrix at 77 K (for details see Experimental Section). A well-defined isosbestic point occurs at 558 nm for the transformation, and the final spectrum is nearly identical to that obtained after ionization of SBV in the same medium, barring two weak bands between 520 and 550 nm which are due to small amounts of a secondary photoproduct, 1,4-dihydropentalene radical cation.[6] Similarly, Figure 2 provides ESR evidence for the photoconversion of $COT^{\bullet+}$ to $BOD^{\bullet+}$, the characteristic and well-resolved hyperfine structure [a(2H) = 36.2 G, a(4H) = 7.7 G] of the photoproduct in spectrum (b) being identical with that displayed in pattern (c) obtained after ionization of SBV. Below we will discuss the assignment of these spectra in terms of the electronic and molecular structure of their proposed carriers and use quantum chemical calculations to substantiate our qualitative MO arguments.

† Institute of Physical Chemistry, University of Fribourg.
‡ Department of Chemistry, University of Tennessee.
§ Present address: Department of Chemistry, California Institute of Technology, Pasadena, CA 91125.
⊥ Present address: Chemical Technology Division, Oak Ridge National Laboratory, Oak Ridge, TN 37831-6181.

⊗ Abstract published in *Advance ACS Abstracts,* July 1, 1995.

(1) (a) Scott, L. T.; Jones, M. *Chem. Rev.* **1972**, *72*, 181; (b) Hassenrück, K.; Martin, H-D.; Walsh, R. *Chem. Rev.* **1989**, *89*, 1125.
(2) Williams, F. *J. Chem. Soc., Faraday Trans.* **1994**, *90*, 1681.
(3) (a) Dai, S.; Wang, J. T.; Williams, F. *J. Am. Chem. Soc.* **1990**, *112*, 2837. (b) Dai, S.; Wang, J. T.; Williams, F. *J. Am. Chem. Soc.* **1990**, *112*, 2835.
(4) Shida, T.; Iwata, S. *J. Am. Chem. Soc.* **1973**, *95*, 3473.
(5) Bally, T. In *Radical Ionic Systems*; Kluwer Academic Press: Dordrecht, 1991; Chapter 1.
(6) Bally, T.; Truttmann, L.; Dai, S., Wang, J. T.; Williams, F. *Chem. Phys. Lett.* **1993**, *212*, 141. Bally, T.; Truttmann, L.; Wang, J. T.; Williams, F. **1995**, *117*, 7923.

0002-7863/95/1517-7916$09.00/0

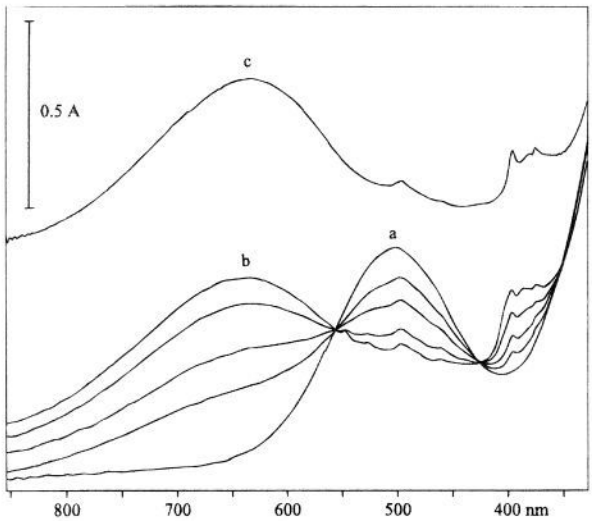

Figure 1. EA spectrum of ionized cyclooctatetraene (a) in a Freon mixture at 77 K and its change upon stepwise monochromatic irradiation at 500 nm (b). The matching spectrum (c) is due to $BOD^{\bullet+}$ as obtained by ionization of SBV.

3. Discussion

3.1. Electronic and Molecular Structure of $COT^{\bullet+}$. The electronic structure of $COT^{\bullet+}$ has been discussed originally by Eland et al.[7a] and later again by Heilbronner et al.[7b] on the basis of the photoelectron (PE) spectrum of COT, and finally by Dunbar et al. on the basis of the photodissociation (PD) spectrum.[7c] Heilbronner et al. used an *ad hoc* parametrized Hückel-type LCBO-model (linear combination of bond orbitals) to draw inferences about the conformation of neutral COT from the first three vertical ionization energies which correspond to ejection of an electron from the π_4-HOMO ($5a_1$: -8.42 eV), from the degenerate $\pi_{2/3}$-MO ($7e$: -9.78 eV), and from the π_1-MO ($4b_2$: -11.15 eV).

By virtue of the fourfold symmetry of COT, the orbital energy differences $\Delta\epsilon_{43} = \epsilon(\pi_4)-\epsilon(\pi_{2/3})$ and $\Delta\epsilon_{21} = \epsilon(\pi_{2/3})-\epsilon(\pi_1)$ are identical and equal to two times the off-diagonal matrix element B_{ab} in the LCBO secular determinant. Indeed, the PE spectrum of COT shows vertical ionization energy differences $\Delta I_{21} = \Delta I_{32} = 1.37$ eV and hence $B_{ab}(\text{LCBO}) = 0.68$ eV. From the relation $B_{ab}(\theta) = B_0 \cdot \cos\theta$ (where θ is the dihedral angle between adjacent π-bonds) and $B_0 = -1.31$ eV for coplanar π-bonds, Heilbronner et al. deduced $\theta(\text{COT}) = 59°$, in excellent agreement with electron diffraction results.[8]

It had already been pointed out by Fu and Dunbar[7c] that the energy corresponding to λ_{max} of the first electronic transition in $COT^{\bullet+}$ (2.55 eV in their gas-phase PD spectrum, 2.45 eV in the present solid-state spectra) is in very poor agreement with $\Delta I_{21} = 1.37$ eV from the PE spectrum of COT which "raises very serious doubts as to whether the structure of the $C_8H_8^{\bullet+}$ ion from COT actually retains the COT structure".[7c] However, it is not necessary to postulate any profound rearrangement to reconcile the PE and PD/EA-data in this case: due to the nodal properties of the π-HOMO, ionization of COT leads to an increase of the π bond orders along the essential single bonds (p_s) and a commensurate decrease along the double bonds (p_d). This expresses itself in the form of an enhancement of the driving force for planarization of COT (as is typical for twisted conjugated π-systems). However, the resulting decrease in π-energy is opposed by a concomitant increase in σ-strain so

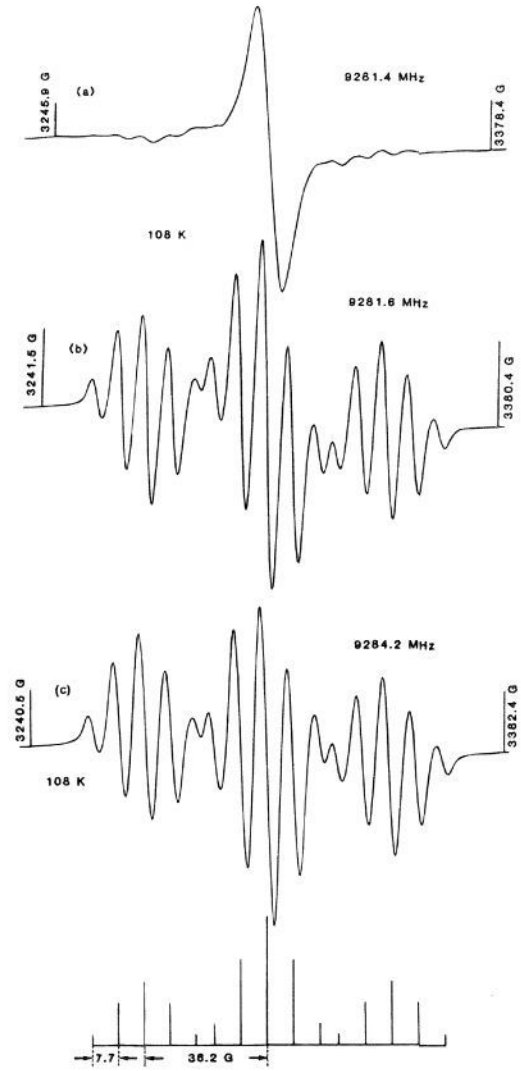

Figure 2. ESR spectrum of ionized cyclooctatetraene (a) in a CF_2-$ClCFCl_2$ matrix at 108 K and its change upon irradiation at $\lambda > 480$ nm (b). The matching spectrum (c) is due to $BOD^{\bullet+}$ as obtained by *ionization of SBV*.

Scheme 1.[a]

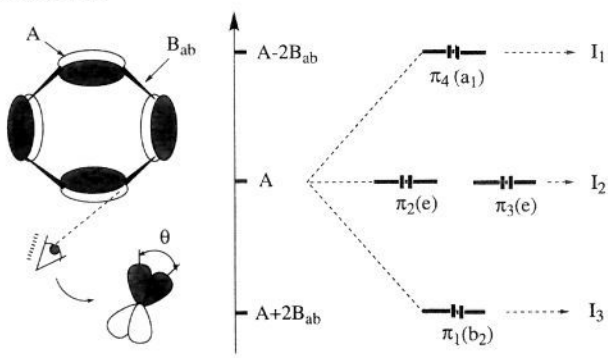

[a] Symmetry labels in D_{2d}.

(7) (a) Eland, J. H. D. *Int. J. Mass Spectrom. Ion Phys.* **1969**, *2*, 471. (b) Batich, C.; Bischof, P.; Heilbronner, E. *J. Electron Spectrosc. Relat. Phenom.* **1972**, *1*, 333. (c) Fu, E. W.; Dunbar, R. C. *J. Am. Chem. Soc.* **1978**, *100*, 2283. In a later, pulsed PD experiment the band at ≈500 nm no longer appeared in the spectrum of $COT^{\bullet+}$, presumably due to rearrangement of the parent cation under these conditions. (Dunbar, R. C.; Kim, M. S.; Olah, G. A. *J. Am. Chem. Soc.* **1979**, *101*, 1368).

(8) (a) Traetteberg, M. *Acta Chim. Scand.* **1966**, *20*, 1724. (b) There are simple relationships between the bond angle α, the folding angle ω (cf. Figure 3), and the dihedral angle θ in an eight-membered ring of D_{2d} symmetry: $\cos\theta = \cos^2\omega = \text{ctg}^2\alpha$.

Table 1. Calculated and Experimental Structures of COT ($^1A_1$) and COT$^{\bullet+}$ ($^2A_1$)

		SCF/6-31G*[a]	MP2/6-31G*[b]	experiment
$^1A_1$	energy	−307.52422[c]	−308.52706[c]	71.1[d,e]
	r(C=C)	1.320	1.348	1.340[f]
	r(C−C)	1.478	1.470	1.476[f]
	α(C=C-C)	127.34	125.94	126.1[f]
	θ[h]	54.4	58.3	57.9[f]
$^2A_1$	energy	−307.276143[c]	−308.25880[c]	≤255.6[d,e,i]
	r(C=C)	1.356	1.376	1.365[j]
	r(C−C)	1.436	1.437	1.451[j]
	α(C=C-C)	132.01	130.70	125.8[j]
	θ[h]	35.8	42.3	≈ 39[k]/56.3[j]

[a] UHF for COT$^{\bullet+}$. [b] UPM2 for COT$^{\bullet+}$ ($\langle S^2\rangle = 0.775$). [c] Total energy in hartree. [d] $\Delta H_f°$ in kcal/mol. [e] Reference 10. [f] Electron diffraction.[8a] [h] Dihedral angle between neighboring C=C bonds.[8b] [i] With $I_a \leq 8.0$ eV. [j] Average values from crystal structure of peralkylated radical ion salt.[12] [k] From the LCBO model (see text).

Table 2. Results of Quantum Chemical Calculations on Excited States of COT$^{\bullet+}$

	method					
	(7,8) CASSCF[a]		(7,8) CASPT2[b]		experiment	
	neutral[c,j]	cation[d,j]	neutral[c,j]	cation[d,e,j]	neutral[f,j]	cation[g,j]
$\Delta E(^2A_1 \rightarrow {}^2A_2)$	3.50	1.45	3.28	1.38 (0)	*h*	*i*
$\Delta E(^2A_1 \rightarrow {}^2E)$	1.24	2.64	1.42	2.66 (0.092)	1.37	2.45
$\Delta E(^2A_1 \rightarrow {}^2B_2)$	2.95	4.27	2.50	3.92 (0.014)	2.75	>3.50

[a] CASSCF calculations including 7 π-electrons in 8 π-MOs. [b] MBPT[2] calculations on the basis of the CASSCF wave functions. [c] Experimental geometry;[8a,15] E_{tot}(CASSCF) = −307.345 747 h; E_{tot}(CASPT2) = −308.259 866 h. [d] MP2/6-31G* optimized geometry; E_{tot}(CASSCF) = −307.375 527 h E_{tot}(CASPT2) = −308.281 449 h. [e] Oscillator strengths in parentheses. [f] From PE spectrum of COT.[7] [g] From EA spectrum of COT$^{\bullet+}$ (Figure 1). [h] Non-Koopmans state, not visible in PE spectrum. [i] Dipole-forbidden transition. [j] Geometry.

that the radical cation may perhaps not achieve a completely planar structure (vide infra).

If we assume that COT does indeed retain its structure upon ionization, the resulting degree of planarization, as measured by the twisting angle θ,[8b] can be deduced from the EA spectrum of COT$^{\bullet+}$ because λ_{max} (≙2.45 eV) corresponds to $\Delta I_{21} = 2B_{ab}$ *at the equilibrium geometry of the cation.* However, we also have to take into account that B_0 increases upon ionization, in proportion to the π-bond order along the essential single bonds (p_s).[9a] In planar polyenes this increase is by ≈20%;[9b] hence we take B_0(COT$^{\bullet+}$) = −1.31·1.2 = −1.57 eV. Assuming that the cos θ relationship holds also in the cation we can derive θ(COT$^{\bullet+}$) ≈ 39°, i.e., a decrease from the value in neutral COT$^{\bullet+}$ by ≈20°.

This semiquantitative prediction is confirmed by quantum chemical calculations whose results are collected in Table 1. The bond lengths and bond angles in neutral COT are predicted very accurately (±0.8 pm; ±0.1°) by the MP2/6-31G* model, while at the SCF level the double bonds are too short by the usual amount (2 pm), and the ring is slightly too flat. The predicted lengthening of the double bonds and the shortening of the single bonds upon ionization is more pronounced at the SCF (+3.6/−4.2 pm) than at the MP2 level (+2.8/−3.3). Concomitantly, the flattening of the ring upon ionization as measured by the dihedral angle θ[8b] is stronger at the SCF level (Δθ = −18.6°) than by MP2 (Δθ = −16.0°). It is satisfying to note that θ calculated at the MP2 level is in good agreement with that deduced above from the optical spectrum by the simple LCBO model.

Thus, oxidation of COT leads to *partial* planarization of the ring, in contrast to reduction which leads to *complete* planarization.[11] However, optimization of planar COT$^{\bullet+}$ at the UMP2/6-31G* level led to a D_{4h} species only 4.4 kcal/mol above the ion's equilibrium structure, thus indicating a very small barrier to ring inversion. Finally, the relaxation energy of COT$^{\bullet+}$ formed vertically (i.e., at the geometry of the neutral) was calculated to be 0.5 eV, in good agreement with $I_v - I_a$ in the first PE band of COT.[7]

We have also calculated the energies of the first few excited states of COT$^{\bullet+}$ both at the neutral (experimental)[8a,15] and at the cation geometry (UMP2/6-31G*) with the CASSCF/CASPT2 procedure[16] (cf. Table 2). This method, which was recently shown to give very reliable results for polyene radical cation excited states,[17] gives excellent agreement with the vertical $^2A_1 \rightarrow {}^2E$ (HOMO-1 → HOMO) transition ($I_{v,2} - I_{v,1}$) at the (experimental) neutral geometry. At the cation geometry, the predicted excitation energy is too high by 0.21 eV which may be an indication that the calculated conformation may be slightly in error or that this state is shifted to lower energy by solvation, as indicated by the gas-phase PD spectrum where the vertical transition energy was reported to be 2.55 eV.[7c] Conversely, the $^2A_1 \rightarrow {}^2B_2$ (HOMO-2 → HOMO) energy difference appears to be underestimated by 0.25 eV, but the exact determination of $I_{v,3}$ in the PE spectrum is difficult and may leave room for an error of this magnitude. Not much can be said about the position of this excited state in COT$^{\bullet+}$ except that it must lie below 350 nm (>3.5 eV) in the EA spectrum.

Interestingly, the calculations predict that the *lowest* excited state ($^2A_2$) at the cation geometry arises from HOMO → LUMO excitation, which at first sight seems surprising because only few cases are known where this state lies below the first Koopmans excited state.[18,19] However, from the nodal proper-

(9) (a) As θ is independent of the absolute values of the π basis energies A in COT (Scheme 1) we can neglect the decrease in p_d upon ionization. (b) Because planar COT has an antiaromatic π system, its p_s (which is actually zero in the LCBO approximation) cannot serve as a reference. Instead we look at the increase from $p_s \approx 0.5$ as is typical in linear conjugated polyenes, to ≈0.6 in the corresponding radical cations.

(10) Pedley, J. B.; Naylor, R. D.; Kirby, S. P. *Thermoechemical Data of Organic Compounds*, 2nd ed.; Chapman & Hall: London, 1986.

(11) (a) Kimmel, P. I.; Strauss, H. L. *J. Phys. Chem.* **1968**, *72*, 2813 and references cited therein. (b) Smentowski, F. J.; Stevenson, G. R. *J. Am. Chem. Soc.* **1968**, *90*, 4661. (c) Hammons, J. H.; Hrovat, D. A.; Borden, W. T. *J. Am. Chem. Soc.* **1991**, *113*, 4500. (d) Samet, C.; Rose, J. L.; Piepho, S. B.; Laurito, J.; Andrews, L.; Schatz, P. N. *J. Am. Chem. Soc.* **1994**, *116*, 11109.

(12) Recently the structure of the $SbCl_6^-$ salt of a peralkylated COT$^{\bullet+}$ derivative has been determined,[13a] but the comparison of this structure with our calculated values is difficult because the counterion and the lattice forces induce quite pronounced dissymmetry,[13b] and because flattening of the ring in this compound appears to be prohibited by steric constraints.[13c]

(13) (a) Nishinaga, T.; Komatsu, K.; Sugita, N.; Lindner, H. J.; Richter, J. *J. Am. Chem. Soc.* **1993**, *114*, 11642. (b) In this salt the C=C bond lengths vary between 1.338 and 1.389 Å and those for the C−C bonds between 1.440 and 1.464 Å. (c) The values for θ which lie between 52.12 and 58.51° (θ_{av} = 56.3°) indicate that a flattening of the ring upon ionization is insignificant compared to the corresponding neutral (θ_{av} = 56.9° from ω_{av} = 42.35°).[14] Interestingly, λ_{max} of this cation is at significantly lower energy (1.67 eV vs 2.45 eV in parent COT$^{\bullet+}$) and much closer to ΔI_{21} of COT (1.37 eV) as a consequence of the prevented flattening of the ring.

(14) Komatsu, K.; Nishinaga, K.; Aonuma, S.; Hirosawa, C.; Takeuchi, K.; Lindner, H. J.; Richter, J. *Tetrahedron Lett.* **1991**, *32*, 6767).

(15) As the dihedral angles to the hydrogen atoms are not given in the electron diffraction data,[8a] these were optimized by MP2/6-31G* while fixing the remaining geometrical parameters at the experimental values. A value of 184° resulted.

(16) (a) Andersson, K.; Malmqvist, P.-Å.; Roos, B. O.; Sadlej A. J.; Wolinski, K. *J. Phys. Chem.* **1990**, *94*, 5483. (b) Andersson, K.; Malmqvist P.-Å. ; Roos, B. O. *J. Chem. Phys.* **1992**, 96, 1218.

(17) Fülscher, M.; Bally, T.; Matzinger, S. *Chem. Phys. Lett.* **1995**, *236*, 167.

(18) The CASSCF calculations showed that the $^2E_2$ and the $^2A_2$ excited state are described to 87% and 90%, respectively, by the lowest energy configurations of their symmetry; hence it is appropriate to argue in terms of a one-electron MO picture in this case.

(19) See, for example: (a) Forster, P.; Gschwind, R.; Haselbach, E.; Klemm, U.; Wirz, J. *Nouv. J. Chim.* **1980**, *4*, 365. (b) Bally. T.; Neuhaus, L.; Nitsche, S.; Haselbach, E.; Janssen, J.; Lüttke, W. *Helv. Chim. Acta* **1983**, *66*, 1288. (c) Kesper, K.; Münzel, N.; Pietzuch, W.; Specht, H.; Schweig, A. *J. Mol. Struct (Theochem)* **1989**, *200*, 375.

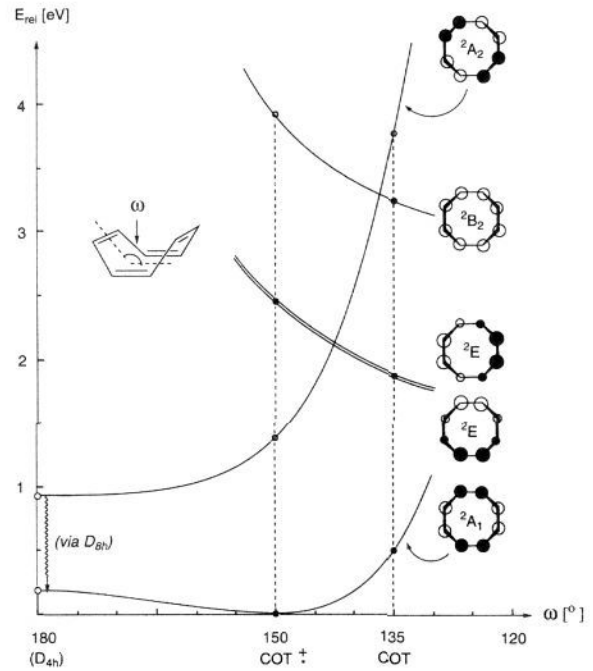

Figure 3. Energies of different states of $COT^{\bullet+}$ as a function of the folding angle ω. Numbers are from experiment (PE/EA spectra, filled circles) or from CASPT2 calculations (open circles, cf. Table 1). The energies at 180° are from RMP2/6-31G*//ROHF/6-31G* calculations. Note that the $^2A_2$ excited state ($^2B_2$ state in D_{4h} symmetry) undergoes activationless decay to the $^2A_1$ ground state ($^2B_1$ in D_{4h}).[20]

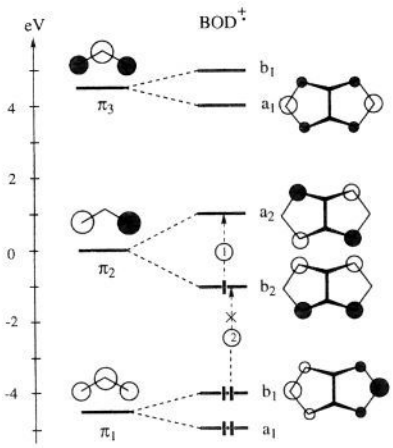

Figure 4. The π-MO's of $BOD^{\bullet+}$ as linear combinations of allyl π-MOs.[22] (See Figure 6 for pictorial representations of the resulting MOs and the text for discussion).

ties of the frontier MOs of COT it follows that the HOMO(a_1)−LUMO(a_2) gap narrows upon flattening of the ring. At the geometry of the radical cation this flattening is apparently sufficient to make the $^2A_2$ HOMO → LUMO excited state the lowest one. Perhaps the corresponding optical transition can be made weakly allowed and hence detectable by EA spectroscopy through appropriate substitution of COT to confirm this interesting prediction experimentally.

Combining the above experimental and theoretical findings allows us to construct the schematic potential energy surface diagram depicted in Figure 3 which shows how the energies of the different states of $COT^{\bullet+}$ change as a function of the folding angle ω.[8b] From this we gather that population of the first excited state of $COT^{\bullet+}$ ($^2A_2$) is expected to lead to rapid conversion to the ground state by way of a planar structure.[20] Conversely, the ^2E state has a tendency to relax to structures

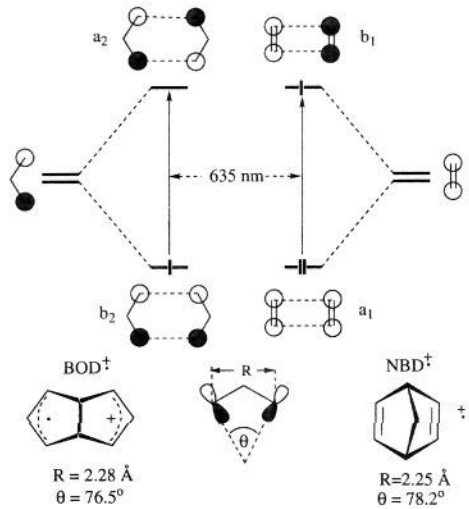

Figure 5. Comparison of the electronic structure of $BOD^{\bullet+}$ and $NBD^{\bullet+}$. R and θ are from RMP2/6-31G* geometry optimizations.

with decreased ω, a feature which will be very important for the photochemistry of $COT^{\bullet+}$ discussed in section 4.

3.2. Electronic Structure of $BOD^{\bullet+}$. Whenever there exists a viable possibility to spatially separate spin and charge in a radical ion, the question arises whether (or, rather, to what extent) such a localization prevails in any given case. Since there is no reason to assume *a priori* that either full localization or full delocalization of spin and charge lead to optimal stabilization of $BOD^{\bullet+}$, we must try and assess the degree of (de)localization in this compound by some experimental and/or theoretical means. This undertaking turned out to be quite involved and will be at the focus of a separate paper.[21] For the purpose of discussing excited states of $BOD^{\bullet+}$ it suffices to state here that by virtue of the strong interaction between the allylic moieties, the ground state $BOD^{\bullet+}$ has true C_{2v} symmetry, i.e., spin and charge are fully delocalized in this system, as it appears in the ESR spectrum.

Thus, interaction between the two allylic moieties will lead to a symmetric splitting of their π-MOs such that all levels are doubled, as shown in Figure 4.[22] Upon accommodating five π-electrons, the positive combination of the nonbonding allyl-MOs will be the HOMO (b_2) and their negative combination the LUMO (a_2). Two possibilities exist for the lowest energy transition, but as one of them ($b_1 \rightarrow b_2$ excitation (2)) is dipole forbidden, it is expected that the lowest energy EA band will arise from HOMO → LUMO electron promotion (1) ($^2B_2 \rightarrow {}^2A_2$, x-polarized).

From Figure 1 we obtain $\lambda_{max}(BOD^{\bullet+}) = 635$ nm which happens to be identical to λ_{max} of the $^2B_1 \rightarrow {}^2A_1$ transition in

(20) The $^2A_2$ excited state ($^2B_2$ in D_{4h} symmetry) will undergo activationless decay to the $^2A_1$ ground state ($^2B_1$ in D_{4h}) by bond shift via a D_{8h} structure (Jahn-Teller active ^2E_g state) where the HOMO and LUMO are degenerate.

(21) Williams, F.; Dai, S; Bally, T.; Truttmann, L. manuscript in preparation.

(22) The energy separation of the MOs in allyl radical can be estimated from the energies of the first two valence excited states at 3.1 and 5.8 eV.[23] In a first approximation, these are due to first-order symmetrical linear combinations of the configurations arising from $\pi_1 \rightarrow \pi_2$ and $\pi_2 \rightarrow \pi_3$ excitation, and therefore their midpoint (i.e., ≈4.5 eV) can be associated with the π_1/π_2 and π_2/π_3 energy difference. This conforms also quite well with the rule-of-thumb relationship 1β(HMO) ≈ −3 eV. Assuming that the 635 nm transition in $BOD^{\bullet+}$ corresponds to $b_2 \rightarrow a_2$ excitation, this gap was set to ≈2 eV. In this case the splitting of the subjacent b_1 and a_1 MOs should be half as much, i.e., ≈1 eV, because the terminal coefficients at the interacting allyl MOs are $1/\sqrt{2}$ instead of 1/2.

(23) See, for example: Maier, G.; Reisenauer, H. P.; Rohde, B.; Dehmke, K. *Chem. Ber.* **1983**, *116*, 732.

Table 3. Excited states of $BOD^{\bullet+}$ by Calculation and Experiment

		(5,6) CASSCF[a]	(5,6) CASPT2[b]	exp.[c]
1^2A_2	energy[d]	2.46	2.16	1.95
	f[e]	0.237	0.209	strong
	$b_2 \rightarrow a_2$[f]	0.88	0.88	
1^2B_1	energy[d]	2.41	2.45	2.45(?)
	f[e]	0	0	very weak
	$b_1 \rightarrow b_2$[f]	0.81	0.81	
	$a_1 \rightarrow a_2$[f]	0.05	0.05	
	$b_1 + b_2 \rightarrow a_2$[g]	0.05	0.05	
1^2A_1	energy[d]	3.43	3.31	3.10
	f[b]	0.0049	0.0048	weak
	$a_1 \rightarrow b_2$[f]	0.51	0.51	
	$b_2 \rightarrow a_1$[f]	0.17	0.17	
	$b_1 \rightarrow a_2$[f]	0.21	0.21	
2^2A_1	energy[d]	4.88	4.16	>4.0
	f[e]	0.010	0.003	
	$a_1 \rightarrow b_2$[f]	0.03	0.03	
	$b_2 \rightarrow a_1$[f]	0.31	0.31	
	$b_1 \rightarrow a_2$[f]	0.45	0.45	

[a] CASSCF calculation including 5 π-electrons in 6 π-MOs. [b] MBPT[2] calculation based on CASSCF wave function. [c] cf. Figure 1. [d] Relative to $^2B_2$ ground state in eV. [e] Oscillator strength for electronic transition from ground state. [f] Weight of configuration described by the indicated electron excitation(s) from the 1^2B_2 ground configuration $(a_1)^2(b_1)^2(b_2)^1$; see MOs in Figure 5. [g] Doubly excited configuration.

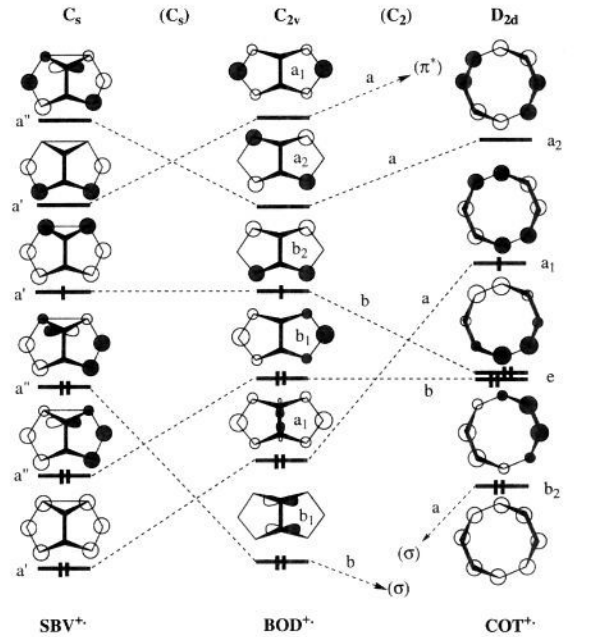

Figure 6. Correlation diagram for the molecular orbitals of the three title cations.

norbornadiene radical cation ($NBD^{\bullet+}$).[24] A comparison of the two systems shows that this may be more than a mere coincidence: in both cases a pair of π-MOs with terminal coefficients of $\sqrt{2}$ are held at a similar angle and distance and are hence expected to experience a similar interaction (cf. Figure 5). The main difference is that in $NBD^{\bullet+}$ the two interacting MOs contain a total of three electrons and in $BOD^{\bullet+}$ only one. Note that the resemblance of the two spectra extends even to the *shape* of the EA bands which is also not surprising because the electronic transition is in both cases between the bonding and the antibonding combination of the respective π-MOs and therefore similar geometry changes are expected upon excitation.

Regarding *higher excited states* of $BOD^{\bullet+}$ we note the occurrence of a small peak at 500 nm and a slightly stronger structured band with $\lambda_{max} = 400$ nm in the spectrum. It appears tempting to assign the first of these to the dipole-forbidden $^2B_2 \rightarrow {}^2B_1$ electronic transition (2) which may gain some intensity through vibronic coupling. The CASPT2 model, which gives very good agreement with experiment for the first excited state (Table 3), indicates that this interpretation may indeed be correct: It predicts the corresponding transition at 2.45 eV while the first $^2B_2 \rightarrow {}^2A_1$ excitation is at 3.31 eV and hence corresponds probably to the 400 nm band system. This is in contrast to our earlier CIS- calculations[6] which had placed the $^2B_1$ *above* the lowest $^2A_1$ state and may serve as an indication that taking only singly excited configurations into account in excited state calculations of radical ions can lead to erroneous state orderings. Indeed, the $(a_1)^2(b_1)(a_2)^2$ doubly excited configuration makes a ≈5% contribution to the CASSCF wave function of the 1^2B_1 state, and its neglect in the CIS model may explain the discrepancy.

4. The Formation of $BOD^{\bullet+}$ from SBV and from $COT^{\bullet+}$. *Symmetry Considerations.* It had been noted by Williams et al. that upon ionization of SBV the only product observed is the radical cation of BOD. The present evidence supports this conclusion in that the EA spectrum observed after radiolysis of SBV is almost indistinguishable from that obtained after 650 nm photolysis of $COT^{\bullet+}$ and assigned above to $BOD^{\bullet+}$. There is ample precedent for cyclopropane moieties undergoing ring opening upon ionization,[25] and in fact a CIDNP investigation on barbaralane was interpreted in terms of a very similar rearrangement to form a bisallylic cation after photoinduced electron transfer.[25b]

It can easily be shown that the $SBV^{\bullet+} \rightarrow BOD^{\bullet+}$ reaction is formally a symmetry allowed process because the singly occupied HOMOs correlate along a C_s reaction coordinate as shown in Figure 6 (left hand side). In fact, all attempts to find a potential energy minimum corresponding to $SBV^{\bullet+}$ by semiempirical or ab initio SCF methods resulted in spontaneous rearrangement to $BOD^{\bullet+}$ (at the equilibrium geometry of neutral SBV, the cation lies 33 kcal/mol higher in energy than $BOD^{\bullet+}$).[6]

More intriguing is the photochemical formation of $BOD^{\bullet+}$ from $COT^{\bullet+}$. Williams et al. had pointed out that the ground states of the two cations are of different symmetry with respect to the common twofold axis, but that one component of the ^2E π-excited state which gives rise to the 505 nm absorption band of $COT^{\bullet+}$ correlates with the HOMO of $BOD^{\bullet+}$ (cf. Figure 6). On this basis it was postulated that this rearrangement represents the first example of a photochemically allowed pericyclic reaction of a radical cation.[3b]

Although this is formally correct, it leaves some interesting questions open: firstly, our above calculations strongly suggest that the ^2E state is actually the *second* excited state of $COT^{\bullet+}$; therefore, if the photochemical reaction were to proceed adiabiatically from this state, it would do so in violation of Kasha's rule. Secondly, the $COT^{\bullet+} \rightarrow BOD^{\bullet+}$ rearrangement requires very pronounced geometry changes for which there must be a driving force. Thirdly, the reverse photoreaction from the $^2A_2$ or $^2A_1$ excited states of $BOD^{\bullet+}$ is symmetry allowed by the same token but is not observed in practice. In order to find answers to these questions we proceeded to explore the potential energy sufaces interconnecting the two reactants by ab initio quantum chemical methods.

Calculations of Potential Energy Surfaces. It was already shown in section 3.1 that optical excitation of $COT^{\bullet+}$ leads to the ^2E excited state and that internal conversion to the lower lying $^2A_2$ state is not expected to lead to any net photochemistry due to rapid relaxation of the latter to the planar cation. As

(24) Haselbach, E.; Bally, T.; Lanyiova, Z.; Baertschi, P. *Helv. Chim. Acta* **1979**, *62*, 538.

(25) (a) Roth, H. D.; *Acc. Chem. Res.* **1987**, *20*, 343. (b) Roth, H. D.; Abelt, C. J. *J. Am. Chem. Soc.* **1986**, *108*, 2013.

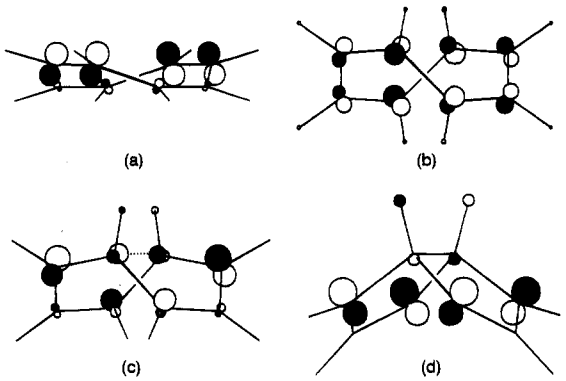

Figure 7. Change in the shape of the singly occupied MO in the course of the $COT^{\bullet+} \rightarrow BOD^{\bullet+}$ interconversion (Moplot representation): (a) One component of the e-MO at the $^2A_1$ equilibrium geometry; (b) D_2 stationary point on JT surface (cf. Figure 8); (c) transition state for $^2B_3 \rightarrow BOD^{\bullet+}$ conversion (cf. Figure 8); and (d) $BOD^{\bullet+}$.

$COT^{\bullet+}$ experimentally shows quite efficient photoconversion to $BOD^{\bullet+}$, another process must compete effectively with internal conversion from the ^2E state. Jahn-Teller (JT) distortion appears as an attractive candidate for this process, and thus we decided to investigate the corresponding relaxation(s).

According to group theory, modes of b_1 and b_2 symmetry lead to first-order JT stabilization in degenerate states of D_{2d} symmetry.[26] The first of these lowers the symmetry to D_2 and the second to C_{2v}. Optimization of the ^2E state of $COT^{\bullet+}$ within these symmetries at the ROHF/6-31G* level[27] led to stationary points 1.68 (C_{2v}) and 1.84 eV (D_2), respectively, below the D_{2d} conical intersection. Single point RMP2 calculations changed these stabilization energies to 1.15 and 1.82 eV, respectively. Thus, first-order JT distortion of ^2E excited $COT^{\bullet+}$ puts the system onto a very steep potential energy surface sloping downward in the direction of increasing ring folding (Figure 3) and which leads to strong stabilization. This may explain why internal conversion to the $^2A_2$ state (and subsequently to the ground state) is inefficient in optically excited $COT^{\bullet+}$.

Most interestingly, the $^2A_1$ ground state of $COT^{\bullet+}$ has risen $\approx$1 eV above the $^2B_3$ state at the D_2 stationary point and is nearly degenerate with the $^2B_2$ state at the C_{2v} stationary point.[28] Consequently, the pronounced Jahn-Teller distortion of ^2E excited $COT^{\bullet+}$ along the b_1 mode leads to a change in ground state symmetry[29] which in view of the conversion to $BOD^{\bullet+}$ corresponds to a *direct passage onto the ground state surface of the photoproduct.* Concomitantly, $COT^{\bullet+}$ makes *significant structural progress* along the reaction coordinate as evidenced by the shortening of the C_1-C_5 distance from 3.356 Å at the ground state geometry to 2.684 Å at the D_2 stationary point.

Second derivative calculations at the ROHF level revealed that neither of the above stationary points are minima on the global potential energy surface. The D_2 "minimum" is actually

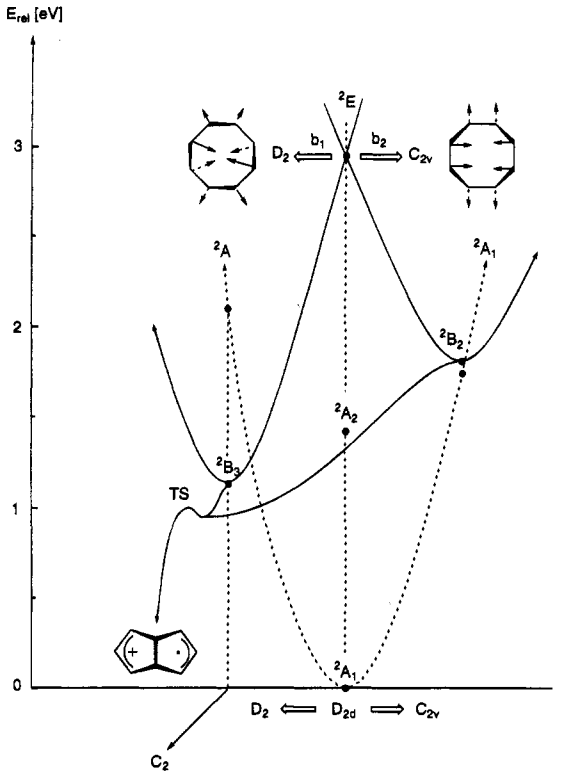

Figure 8. Potential energy curves for the Jahn-Teller distortion of ^2E excited $COT^{\bullet+}$ and its subsequent rearrangement to $BOD^{\bullet+}$. Relative energies are from RMP2/6-31G*//ROHF/6-31G* calculations whose results are summarized in Table 4. Discussion see text.

a second order saddle point with imaginary normal modes[30] of b_1 and b_2 symmetry, respectively, leading to two structures of C_2 symmetry. Relaxation along these modes led to marginal stabilization (1.41 and 0.02 kcal/mol, respectively) at the ROHF level, but as the ROMP2 energy was $\approx$1 kcal/mol higher for these new stationary points, this distortion may be an artefact of the single-determinant model. The C_{2v} structure corresponds to a transition state with an imaginary normal mode of b_1 symmetry. Surprisingly, relaxation along this mode led to the same stationary point as obtained from the D_2 structure along the b_1 imaginary mode. The C_{2v} relaxation appears to be real as it is accompanied by a 10 kcal/mol stabilization even at the RMP2 level.

Although $COT^{\bullet+}$ has moved strongly in the direction of $BOD^{\bullet+}$ during the JT distortion of the ^2E state (and the ensuing stabilization of the C_{2v} stationary point), it does not spontaneously decay to the product. The reason for this becomes evident by inspection of the HOMO and its change along the reaction coordinate (see Figure 7): although it is of the proper symmetry, the antibonding character it retains along the C_1-C_5 linkage at the D_2 stationary point must be compensated by bonding interactions in the lower orbitals before the system attains a downhill part of the potential surface. By shrinking the C_1-C_5 distance one arrives at a C_2 transition state on the ROHF surface, 3.2 kcal/mol above the D_2 stationary point (1 kcal/mol below by single-point ROMP2 calculations), where the coefficients at C_1 and C_5 have already diminished considerably and at the same time the coefficients at C_3 and C_7 (which become zero by symmetry in $BOD^{\bullet+}$) have nearly disappeared. After crossing this small barrier, the system relaxes spontaneously to ground state $BOD^{\bullet+}$.

Figure 8 graphically summarizes the results of the above described calculations which have confirmed the prediction of

(26) Herzberg, G. *Molecular Spectra and Molecular Structure, Vol III: Electronic Spectra and Electronic Structure of Polyatomic Molecules*; Van Nostrand Reinhold: New York, 1966, p 50.

(27) Upon distortion from D_{2d} symmetry, very pronounced spin contamination appears in the UHF wave functions. Therefore we resorted to the ROHF model where this problem does not pose itself.

(28) This near degeneracy indicates an (avoided) surface crossing. At such points vibronic mixing becomes important and may cause a certain fraction of the excited $COT^{\bullet+}$ molecules to fall back to the ground state surface before further relaxation, thus reducing the quantum yield for photoproduct formation.

(29) A similar case was encountered a while ago in a bishomotetraazaadamantane radical cation (Nelsen, S. F.; Haselbach, E.; Gschwind, R.; Klemm, U.; Lanyiova, Z. *J. Am. Chem. Soc.* **1978**, *100*, 4367. Haselbach, E.; Bally, T.; Gschwind, R.; Klemm, U.; Lanyiova, Z. *Chimia* **1979**, *33*, 405.).

(30) By this (not entirely correct) term we designate normal modes associated with negative eigenvalues of the Hessian matrix and therefore imaginary frequencies.

Table 4. Energies (in eV) Relative to Ground State $COT^{\bullet+}$ of Stationary Points on the Potential Energy Surface for Jahn-Teller Distortion of ^2E Excited $COT^{\bullet+}$ and Its Subsequent Rearrangement to $BOD^{\bullet+}$ (for a Schematic Representation of RMP2 Results See Figure 8)

state	geometry[a]	ROHF/6-31G*	RMP2/6-31G*
$^2A_1$	$^2A_1$[b]	−307.267969[c]	−308.263549[c]
$^2A_2$	$^2A_1$	+1.85	+1.43
^2E	$^2A_1$	+3.22	+2.96
$^2B_3$	$^2B_3$[d]	+1.38	+1.14
^2A[e]	$^2B_3$	+2.56	+2.12
$^2B_2$	$^2B_2$[f]	+1.54	+1.81
$^2A_1$[e]	$^2B_2$	+2.05	+1.74
$2A''$	$2A''$[g]	+1.52	+1.09

[a] All geometry optimizations at ROHF/6.31G* level. [b] Equilibirum geometry of ground state $COT^{\bullet+}$. [c] Absolute energy in hartree. [d] D_2 stationary point. [e] Corresponding to $^2A_1$ ground state in D_{2d}. [f] C_{2v} stationary point. [g] Transition state for $^2B_3 \rightarrow BOD^{\bullet+}$ conversion in C_2 symmetry.

a diabatic photoreaction from ^2E excited $COT^{\bullet+}$ to ground state $BOD^{\bullet+}$ along a C_2 reaction coordinate. In addition they revealed the reason for the violation of Kasha's rule and also the driving force for this intriguing rearrangement: both are due to the strong JT stabilization and the associated distortion of the ^2E excited state of $COT^{\bullet+}$ along the reaction coordinate leading to $BOD^{\bullet+}$ which competes effectively with internal conversion to the lower-lying $^2A_2$ excited state.

Turning to the third question posed at the outset of this section (why is the—equally symmetry allowed—reverse photoreaction not observed?) we note that the photochemically active $^2A_2$ excited state of $BOD^{\bullet+}$ has an "intended" symmetry correlation with the $(e)^2(a_1)^2(a_2)^1$ configuration of $COT^{\bullet+}$ which corresponds to the highly excited $^2A_2$ state of the product. Instead of following this initial uphill path to $COT^{\bullet+}$, the $^2A_2$ state of $BOD^{\bullet+}$ instead relaxes very efficiently to a much flatter structure with a folding angle between the two five-membered rings of 139°, up from 102° in $^2B_2$ whereas the length of the central bond remains virtually unchanged.[6] Thus, in contrast to $COT^{\bullet+}$, $BOD^{\bullet+}$ does not undergo structural progress along the reaction coordinate leading to cleavage of the central bond after photoexcitation. In fact, this molecule undergoes some quite different photochemistry, i.e., two hydrogen shifts to form the 1,4-dihydropentalene radical cation.[6]

Conclusions

The electronic absorption spectrum indicates that the radical cation of cyclooctatetraene ($COT^{\bullet+}$) is nonplanar, in contrast to the corrsponding radical anion.[11] From qualitative and quantitative MO calculations we obtain an estimate of ≈40° for the dihedral angle between adjacent π bonds, compared to 58° for the parent neutral. Qualitative considerations and ab initio electronic structure calculations show that the lowest excited state of $COT^{\bullet+}$ corresponds to optically forbidden HOMO → LUMO excitation and cannot be involved in the observed photorearrangement of $COT^{\bullet+}$ to the radical cation of bicyclo[3.3.0]octa-2,6-diene-4,8-diyl ($BOD^{\bullet+}$).[3b]

The electronic structure of $BOD^{\bullet+}$ is discussed in terms of an intramolecular complex of two π systems analogous to the radical cation of norbornadiene ($NBD^{\bullet+}$) which happens to show an almost identical UV/vis spectrum. Ab-initio calculations show that the component π-systems in the two compounds are actually at similar angles and distances which explains the similarity of their spectra. The disposition of excited states in $BOD^{\bullet+}$ is dicussed on the basis of CASSCF/CASPT2 calculations.

The $COT^{\bullet+} \rightarrow BOD^{\bullet+}$ photoreaction, which is formally a symmetry allowed process if it proceeds from the ^2E excited state of $COT^{\bullet+}$, was studied in some detail by ab initio calculations. The results show that the driving force for this rearrangement stems from a strong Jahn-Teller distortion of the ^2E excited state of $COT^{\bullet+}$ which represents significant *structural progress towards the product* and which furthermore leads to a *crossing to the product ground state surface*. The same effect is probably responsible for the violation of Kasha's rule, i.e., the efficient competition of the observed photoreaction with internal conversion to the lowest excited state of $COT^{\bullet+}$.

Experimental and Computational Procedures

The EA spectra shown in Figure 1 were obtained after γ-irradiation (≈0.5 Mrad) of 0.005 M solutions of COT or SBV in a 1:1 mixture of CF_3Cl and CF_2BrCF_2Br.[31] Details of the technique are described in ref 5 (section 3.2). The ESR spectra in Figure 2 were similarly obtained after radiolytic oxidation of dilute (0.003 to 0.01 M) solutions of COT and SBV in $CF_2ClCFCl_2$ at 77 K. The general technique for variable-temperature ESR studies of γ-irradiated samples has been described elsewhere.[32] All ab-initio structure calculations were done with the 6-31G* basis set. In order to avoid artefacts due to spin contamination and overestimation of spin polarization, we employed the ROHF procedure. In selected cases ($BOD^{\bullet+}$, $COT^{\bullet+}$ ground state) the structures were refined at the RMP2 level[33] which was, however, too costly to be applied generally. However, single point RMP2 calculations (with frozen core MOs) were done at all stationary points in order to account for correlation effects on the relative energies. The Gamess/US program[34] served for ROHF optimization and RMP2 single point calculations, whereas Cadpac 5.2[35] was used for RMP2 optimizations.

Vertical excited state energies of $COT^{\bullet+}$ and $BOD^{\bullet+}$ were calculated by the recently introduced CASSCF/CASPT2 procedure[16] using the Molcas/2 suite of programs.[36] Thereby, nondynamic correlation between all π-electrons in all π-MOs (5 in 6 for $BOD^{\bullet+}$, 7 in 8 for $COT^{\bullet+}$) was modeled in the complete active space (CAS) part, whereas dynamic correlation of all but the core electrons was accounted for at the MBPT[2] level (PT2). An ANO type basis set of valence double-ζ quality with a single polarization functions was used throughout.[37]

Acknowledgment. This work is part of project No. 2028-040398.94 of the Swiss National Science Foundation. The research at the University of Tennessee was supported by the Division of Chemical Sciences, Office of Basic Energy Sciences, U.S. Department of Energy (Grant No. DE-FG05-88ER13852). We thank Dr. Markus Fülscher (University of Lund, Sweden) for help with the CASSCF/CASPT2 calculations, Dr. J. T. Wang for technical assistance, and Prof. E. Haselbach (University of Fribourg) for his continuing support and encouragement.

JA950852C

(31) Sandorfy, C. *Can. J. Spectrosc.* **1965**, *85*, 10. Grimison, A.; Simpson, G. A. *J. Chem. Phys.* **1968**, *72*, 1776.

(32) Adam, W.; Walter, H.; Chen, G.-F.; Williams, F. *J. Am. Chem. Soc.* **1992**, *114*, 3007.

(33) Knowles, P. J.; Andrews, J. S.; Amos, R. D.; Handy, N, C.; Pople, J. A. *Chem. Phys. Lett.* **1991**, *187*, 21. Procedure as implemented in Cadpac[35] (OSCF/MP2).

(34) (a) Gamess; Schmidt, M. W.; Baldridge, K. K.; Boatz, J. A.; Jensen, J. H.; Koseki, S.; Gordon, M. S.; Nguyen, K. A.; Windus T. L. ; Elbert, S. T. *QCPE Bull.* **1990**, *10*, 52. (b) For the version used in this work, see: Schmidt, M. W.; Baldridge, K. K.; Boatz, J. A.; Elbert, S. T.; Gordon, M. S.; Jensen, J. H.; Koseki, S.; Matsanuga, N.; Nguyen, K. A.; Su, S. J.; Windus, T. L.; Dupuis M.; Montgomery, J. A. *J. Comput. Chem.* **1993**, *14*, 1347.

(35) Cadpac5, the Cambridge Analytical Derivatives package, Issue 5.2, Amos, R. D.; Alberts, I. L.; Andrews, J. S.; Colwell, S. M.; Handy, N. C.; Jayatilake, D.; Knowles, P. J.; Kobayashi, R.; Koga, N.; Laidig, K. E.; Maslen, P. E.; Murray, C. W.; Rice, J. E.; Sanz, J.; Simandiras, E. D.; Stone A. J.; Su, M.-D. Cambridge, 1993.

(36) Molcas, Version 2; Andersson, K.; Blomber, M. R .A.; Fülscher, M. P.; Kellö, V.; Lindh, R.; Malmqvist, P.-Å.; Noga, J.; Olsen, J.; Roos, B. O.; Sadlej, A.; Siegbahn, P. E. M.; Urban M.; Widmark, P.-O. Department of Theoretical Chemistry, Chemical Center, University of Lund, Sweden, 1992.

(37) Widmark, P.-O.; Malmqvist, P.-Å.; Roos, B. O. *Theor. Chim. Acta* **1990**, *77*, 291.